

Status of the MUonE experiment

Pilato R. N.^{1,2*}

1 Università di Pisa, Pisa, Italy
 2 INFN, Sezione di Pisa, Pisa, Italy
 * riccardonunzio.pilato@phd.unipi.it

December 9, 2021

16th International Workshop on Tau Lepton Physics (TAU2021),
 September 27 – October 1, 2021
 doi:[10.21468/SciPostPhysProc.7.01.011](https://doi.org/10.21468/SciPostPhysProc.7.01.011)

Abstract

The latest measurement of the muon $g-2$, recently announced at Fermilab, exhibits a 4.2σ discrepancy from the Standard Model prediction. The hadronic contribution a_μ^{HLO} represents the main source of uncertainty on the theoretical prediction. The MUonE experiment proposes a novel approach to determine a_μ^{HLO} by measuring the effective electromagnetic coupling in the space-like region, via $\mu-e$ elastic scattering. The measurement is performed by scattering a 160 GeV muon beam, available at CERN, on atomic electrons of a low-Z target. A Test Run on a reduced detector is planned in 2022, to validate this proposal. The status of the experiment in view of the Test Run is presented.

Contents

1 Introduction	1
2 The MUonE experimental proposal	3
2.1 Theoretical progress	4
3 Test Run 2021-2022	5
4 Conclusions and future plans	7
References	7

1 Introduction

The muon magnetic anomaly is defined as $a_\mu = (g_\mu - 2)/2$, where g_μ is the gyromagnetic ratio. It is a low energy observable which can be both computed and measured with very high precision, and can be used as a stringent test of the Standard Model. Recently, the E989 Muon $g-2$ Collaboration at Fermilab announced its first result for a_μ [1], which is in excellent agreement with the previous measurement performed by the BNL E821 experiment [2]. The

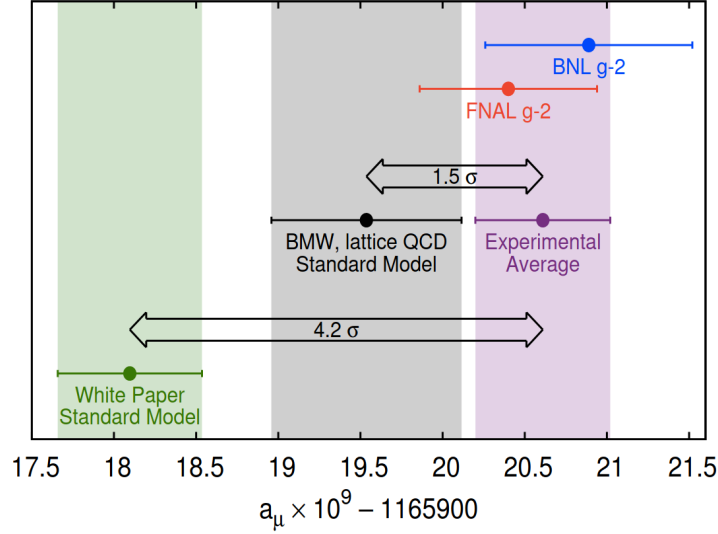


Figure 1: From the top to the bottom: experimental values of a_μ measured by BNL E821 [2], Fermilab E989 [1] and their combined average. Standard Model evaluation of BMW Collaboration using lattice QCD [6] is also shown, as well as the value recommended by the Muon g-2 Theory Initiative [3].

27 combination of the two experimental values leads to a 4.2σ discrepancy with the Standard
 28 Model prediction currently recommended by the Muon g-2 Theory Initiative [3]. Figure 1 rep-
 29 represents the current scenario.

30 In the next years, the accuracy on a_μ will be improved by a factor of 4 by the E989 experi-
 31 ment, reaching the remarkable accuracy of 0.14 ppm [4]. Moreover, a new technique will be
 32 exploited at J-PARC to measure a_μ in an independent way [5]. Therefore, an improvement is
 33 also required on the theoretical prediction, as its uncertainty can become the main limitation
 34 for a test of the Standard Model.

35 The accuracy on the Standard Model calculation is limited by the evaluation of the leading or-
 36 der hadronic contribution a_μ^{HLO} , which cannot be computed perturbatively at low energies. For
 37 this reason, a_μ^{HLO} is traditionally determined by means of a dispersion integral on the annihila-
 38 tion cross section $e^+e^- \rightarrow$ hadrons, which is densely populated by resonances and influenced
 39 by flavour threshold effects. These aspects limit the final precision achievable by this method.
 40 Despite these difficulties, the calculation of a_μ^{HLO} reached an accuracy of $\sim 0.6\%$ [3].

41 In addition to this, a recent evaluation of a_μ^{HLO} based on lattice QCD calculation reached for the
 42 first time an accuracy comparable to the dispersive approach [6]. However, there is a tension
 43 between these two theoretical evaluations. The lattice QCD value weakens the discrepancy
 44 between theory and experiment to 1.5σ , as shown in Figure 1. An independent crosscheck of
 45 a_μ^{HLO} is then required to solve this tension and consolidate the theoretical prediction.

46 MUonE proposes an innovative method to measure a_μ^{HLO} . It based on the direct measurement
 47 of the hadronic contribution to the running of the electromagnetic coupling constant ($\Delta\alpha_{had}$)
 48 in the space-like region [7]. The following equation will be used to calculate a_μ^{HLO} :

$$a_\mu^{HLO} = \frac{\alpha_0}{\pi} \int_0^1 dx (1-x) \Delta\alpha_{had}[t(x)] \quad (1)$$

49 Here, α_0 is the fine structure constant, and the integration variable x is related to the space-like
50 momentum transfer t through the formula

$$t(x) = \frac{x^2 m_\mu^2}{x-1} < 0 \quad (2)$$

where m_μ is the muon mass.

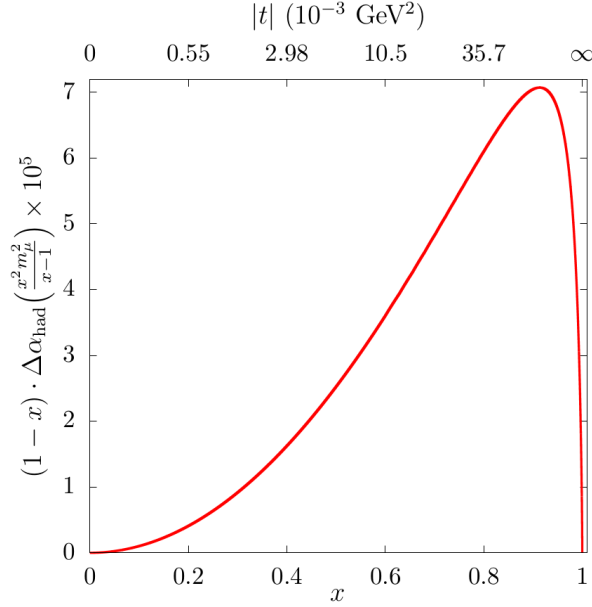


Figure 2: Integrand $(1-x)\Delta\alpha_{had}[t(x)] \times 10^5$ as a function of x and t (upper scale) [8].

51
52 Figure 2 shows the integrand function of the master integral in Eq. 1. The peak of the integrand
53 occurs at $x_{peak} \simeq 0.914$, which corresponds to a momentum transfer $t_{peak} \simeq -0.108 \text{ GeV}^2$.
54 Here, $\Delta\alpha_{had}(t_{peak}) \simeq 7.86 \times 10^{-4}$.
55 The main advantage of this method is that $\Delta\alpha_{had}$ is a smooth function for negative momentum
56 transfer, in contrast with the time-like e^+e^- data used in the traditional dispersive approach. A
57 further advantage is that the electromagnetic running in the region of interest for the evalua-
58 tion of a_μ^{HLO} can be measured by a single scattering experiment. For this reason, the space-like
59 approach is not affected by the systematic uncertainties due to handling data from different
60 experiments, which instead are relevant for the time-like dispersive method. Therefore, the
61 method proposed by MUonE allows a completely independent estimation of a_μ^{HLO} , which can
62 be compared with time-like and lattice QCD results towards a firmer prediction of a_μ .

63 2 The MUonE experimental proposal

64 The MUonE experiment aims to extract $\Delta\alpha_{had}(t)$ from a precise measurement of the shape
65 of the differential cross section of the $\mu^+e^- \rightarrow \mu^+e^-$ elastic scattering [8]. It is performed
66 by scattering a high energy muon beam on the atomic electrons of a low-Z target. A 160
67 GeV muon beam, currently available at CERN M2 beamline, allows to cover the momentum
68 transfer region $-0.153 \text{ GeV}^2 < t < 0 \text{ GeV}^2$, which is equivalent to $0 < x < 0.932$. This
69 corresponds to $\sim 87\%$ of the master integral in Eq. 1. The remaining fraction can be computed
70 by extrapolating $\Delta\alpha_{had}(t)$ with an appropriate parameterization [9]. Furthermore, the simple
71 kinematics of the two-body elastic process makes the scattering angles of the electron and

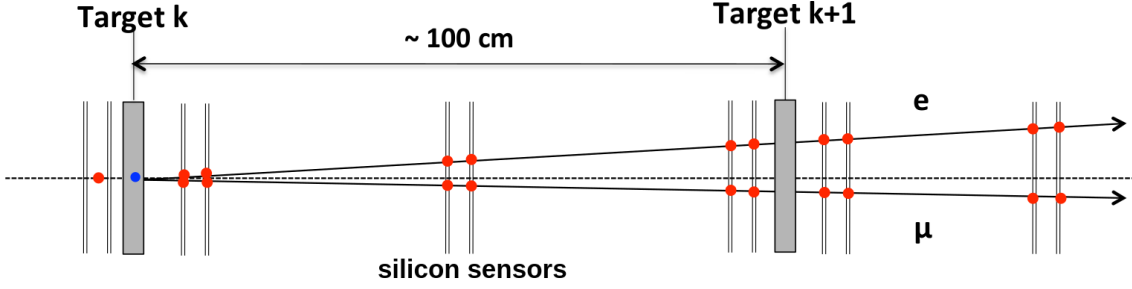


Figure 3: Sketch of a single station (image not to scale).

72 muon correlated. This constraint allows to select elastic events and reject background, which
 73 is expected to be mainly due to e^+e^- pair production by muons in the target. The elastic
 74 scattering kinematics is highly boosted in the forward direction in the laboratory frame, due
 75 to the high energy muon beam employed. This allows to use a single detector to cover the
 76 full acceptance, since the elastic events which are interesting for the experiment are contained
 77 within ~ 32 mrad for the electron and within ~ 5 mrad for the muon.

78 The experimental apparatus consists of a repetition of 40 identical stations. A sketch of a
 79 single station is shown in Figure 3. It is composed of a 15 mm thick Beryllium target followed
 80 by a tracking system with a lever arm of ~ 1 m, which is used to measure the scattering angles
 81 with high precision. The tracking system is composed of 3 pairs of Silicon strip detectors.
 82 Each pair measures both X and Y transverse coordinates, thus strips of the second detector
 83 are orthogonal to the first ones. An electromagnetic calorimeter is placed downstream all the
 84 stations, in order to provide e/μ particle identification in the low angles region. The apparatus
 85 will be also equipped with a muon filter, placed downstream the calorimeter.

86 The modular structure of MUonE allows to re-use the incoming muon beam for each station,
 87 which acts as an independent unit. In this way, $\mu - e$ elastic events will be distributed along
 88 the entire apparatus, increasing the collected statistics but minimizing at the same time the
 89 thickness of a single Beryllium target. This helps to keep under control multiple scattering
 90 effects, which break $\mu - e$ angular correlation.

91 Given the total target thickness of 60 cm and the average intensity of $\sim 1.3 \times 10^7 \mu/s$ of the
 92 CERN M2 beamline, MUonE can reach an integrated luminosity of about $1.5 \times 10^7 \text{nb}^{-1}$ in
 93 3 years of data taking. This is equivalent to collect $\sim 4 \times 10^{12}$ elastic events with electron
 94 energy > 1 GeV, and allows to achieve a statistical error of $\sim 0.3\%$ on a_μ^{HLO} . This makes the
 95 measurement of MUonE competitive with the time-like evaluation.

96 The main challenge of the experiment is to keep the systematic error at the same level of the
 97 statistical one. This is equivalent to measure the shape of the differential cross section with a
 98 systematic accuracy of $\mathcal{O}(10 \text{ ppm})$ at the peak of the integrand function [8]. The most relevant
 99 sources of systematic uncertainties are the longitudinal alignment of a station, which must be
 100 controlled at the level of $10 \mu\text{m}$, the knowledge of the average beam energy, which needs to
 101 be determined with a precision of few MeV [9], and multiple scattering effects. Preliminary
 102 analyses indicate that these effects can be controlled at the required values. Results from a Test
 103 Beam performed at CERN with 12-20 GeV electrons on 8-20 mm C targets show a satisfactory
 104 agreement between data and GEANT4 simulation [10].

105 2.1 Theoretical progress

106 On the theoretical side, the development of high precision Monte Carlo tools is needed, since
 107 the differential cross section must be calculated up to the NNLO to meet the requirement of
 108 $\mathcal{O}(10 \text{ ppm})$ systematic uncertainty. Presently, the full set of NLO QED and electroweak correc-
 109 tions is completed, and a fully exclusive Monte Carlo generator is available [11]. The NNLO

110 hadronic corrections have been computed in [12, 13]. The full set of QED NNLO corrections
 111 is still not yet available, although several important steps have been carried out [14–17]. Two
 112 independent Monte Carlo codes with full NNLO corrections are being developed [18, 19]. Ref-
 113 erence [20] gives a state of art review of the theoretical progress in MUonE. Possible new
 114 physics effects in $\mu - e$ elastic scattering have been investigated in [21, 22], and are expected
 115 to lie below MUonE sensitivity.

116 3 Test Run 2021-2022

117 A Letter of Intent has been submitted to the CERN SPS Committee in 2019 [9], obtaining posi-
 118 tive recommendations. A Test Run of 3 weeks has been approved to validate the experimental
 119 proposal. Due to Covid-19, it has been delayed to 2022. A parasitic run with four Silicon
 120 detectors has been performed at the M2 beamline from 25th October to 15th November 2021.
 121 The Test Run detector will be composed of two full MUonE stations followed by an electro-
 122 magnetic calorimeter. A further tracking station without target will be placed upstream the
 123 apparatus, to detect the incoming muons.

124 The basic tracking unit has been chosen to be the 2S modules developed for the CMS Outer
 125 Tracker upgrade [23]. Figure 4 shows a schematic view of a 2S module. Each module is
 126 composed of 2 close-by Silicon strip sensors with the same dimension and strip orientation,
 127 thus reading the same coordinate. Each sensor is $320\ \mu\text{m}$ thick, with an area of approximately
 128 $10 \times 10\ \text{cm}^2$. Therefore, a single module allows to cover the full angular acceptance, ensuring
 129 a uniform response over all the scattering angles. The two sensors composing a module are
 130 mounted on the same mechanical structure, and are read out by the same front-end electron-
 131 ics, which compares signals from the two sensors to find correlated hits. This feature can be
 132 exploited to reject large angle tracks and suppress background from single sensor hits. The
 133 read-out rate at 40 MHz is capable to sustain the M2 beamline in-spill rate (50 MHz) mini-
 134 mizing the pileup. 2S modules have a single hit resolution of $\sim 20\ \mu\text{m}$, which can be further
 135 improved by rotating a module around the strip orientation. Simulation studies show that a
 136 tilt of $233\ \text{mrad}$ ($\sim 14^\circ$) improves the single hit resolution to $\sim 10\ \mu\text{m}$ keeping a high detection
 efficiency.

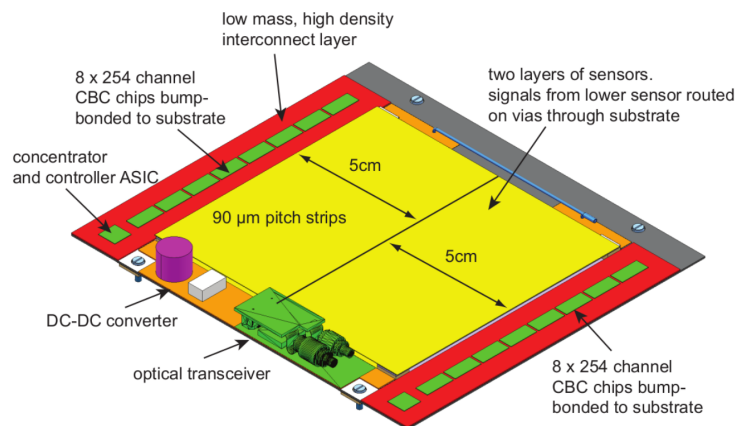


Figure 4: Schematic representation of a 2S module [9].

137

138 The current setup of a MUonE station is represented in Figure 5. First and third pair of 2S
 139 modules are tilted to implement the single hit resolution improvement, while the second pair
 140 is rotated by 45° around the beam axis, in order to solve reconstruction ambiguities. The me-
 141 chanical structure is made of Invar. It is a Fe-Ni alloy which has a low coefficient of thermal

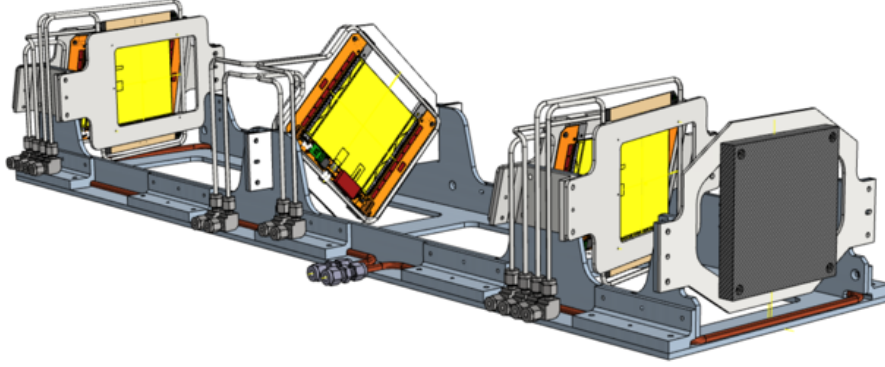


Figure 5: CAD drawing of a MUonE station.

142 expansion ($\sim 1.2 \times 10^{-6} \text{ K}^{-1}$), in order to meet the stringent request of $10 \mu\text{m}$ on the stability
 143 of the longitudinal size. For this purpose, an enclosure and a cooling system have been also
 144 designed to keep the temperature of the station constant within $1 \text{ }^\circ\text{C}$.

145 Presently, an aluminum mockup has been manufactured to test the mechanical structure pla-
 146 narity and the correct integration of the 2S modules. Stepper motors are used to align the sta-
 147 tion with the muon beam. They have been successfully tested in the parasitic run of Fall 2021.

148 The electromagnetic calorimeter used in the Test Run is composed of a matrix of 5×5
 149 PbWO_4 crystals. The total area of $14 \times 14 \text{ cm}^2$ allows to cover the full acceptance for the
 150 scattering events from the two MUonE stations. Each crystal has a section of $2.85 \times 2.85 \text{ cm}^2$
 151 and a length of 22 cm ($\sim 25X_0$), and will be read-out by APD sensors. Tests on sensors and
 152 crystal response are currently ongoing.

153 The Test Run will be mainly aimed at monitoring the mechanical and thermal stability of
 154 the apparatus, as well as confirming the validity of the system engineering. It will be crucial
 155 to test the alignment procedures and check the front-end electronics and the DAQ system.
 156 Data streams from the 2S modules and the calorimeter will be processed by a single Serenity
 157 board [24]. No event selection will be applied during the Test Run. All the information will
 158 be then used to elaborate online selection algorithms to be implemented in the Full Run with
 159 40 stations.

160 Assuming to accomplish these primary goals in the first two weeks of running, the remain-
 161 ing days could be exploited to collect $\sim 5 \text{ pb}^{-1}$ of good quality data, corresponding to $\sim 10^9$
 162 elastic events with electron energy $> 1 \text{ GeV}$. Such a data sample will allow to measure the
 163 leptonic contribution to the electromagnetic running, which is $\lesssim 10^{-2}$ in our kinematic range.
 164 Moreover, it could be enough to get an initial sensitivity to $\Delta\alpha_{had}(t)$, which is $\lesssim 10^{-3}$ in the
 165 MUonE kinematic region. Given the limited statistics which could be collected in the Test Run,
 166 the effect of $\Delta\alpha_{had}(t)$ can be modeled as a linear deviation in t on the shape of the differen-
 167 tial cross section. It can be easily displayed considering the ratio R_{had} between the observed
 168 differential cross section and the theoretical prediction computed assuming only the presence
 169 of the leptonic running. It turns out to be

$$R_{had} \simeq 1 + 2\Delta\alpha_{had}(t) \quad (3)$$

170 Figure 6 shows the expectation of R_{had} obtained using the MUonE NLO Monte Carlo generator.
 171 The extraction of $\Delta\alpha_{had}(t)$ is carried out by means of a template fit method [9]. The resulting
 172 value for the slope of the hadronic running is $K = 0.137 \pm 0.027$.

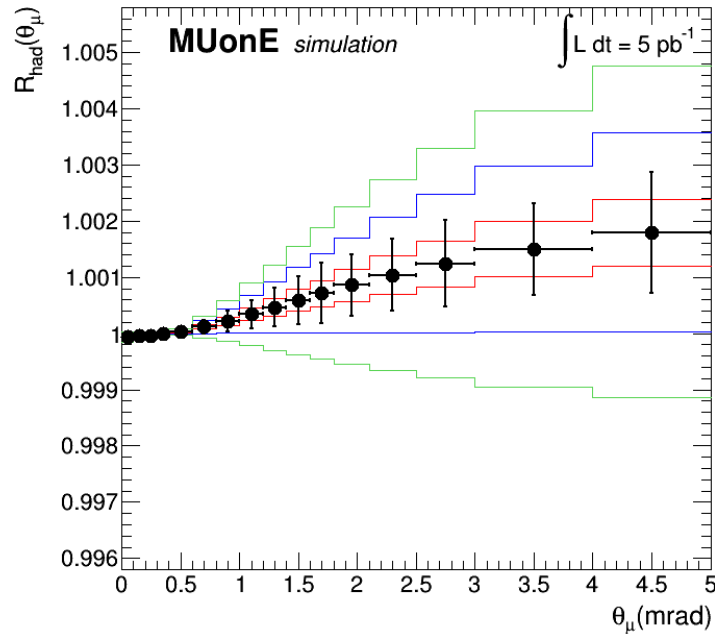


Figure 6: Ratio R_{had} as a function of the muon scattering angle. The error bars correspond to the statistical uncertainties for an integrated luminosity of 5 pb^{-1} . Red, blue and green lines represent templates for different values of the slope of $\Delta\alpha_{had}(t)$.

173 4 Conclusions and future plans

174 At present, the MUonE Collaboration includes collaborators from institutions in China, Greece,
175 Italy, Poland, Russia, Switzerland, UK, USA and at CERN.

176 An intense activity is ongoing for the preparation of the Test Run, which will be a proof of
177 concept of the overall project. If successful, a full proposal will be prepared including support
178 from the results of the Test Run. A first measurement of a_μ^{HLO} could be performed in 2023-24
179 by adding 10 stations to the existing prototype. Preliminary studies show that a running time
180 of 4 months will allow to achieve a $\sim 2\%$ statistical accuracy. A Run with the full detector
181 would be then envisaged in the following years.

182 References

- 183 [1] B. Abi *et al.* (Muon $g-2$ Collaboration) *Measurement of the Positive Muon Anoma-*
184 *lous Magnetic Moment to 0.46 ppm*, Phys. Rev. Lett. **126**, 141801 (2021),
185 doi:[10.1103/PhysRevLett.126.141801](https://doi.org/10.1103/PhysRevLett.126.141801).
- 186 [2] G. W. Bennett *et al.* (Muon $g-2$ Collaboration) *Final report of the E821 muon*
187 *anomalous magnetic moment measurement at BNL*, Phys. Rev. D **73**, 072003 (2006),
188 doi:[10.1103/PhysRevD.73.072003](https://doi.org/10.1103/PhysRevD.73.072003).
- 189 [3] T. Aoyama *et al.* *The anomalous magnetic moment of the muon in the Standard Model*,
190 Physics Reports **887**, 1 (2020), doi:[10.1016/j.physrep.2020.07.006](https://doi.org/10.1016/j.physrep.2020.07.006).
- 191 [4] J. Grange *et al.* (Muon $g-2$ Collaboration) *Muon ($g-2$) Technical Design Report*, (2015)
192 <https://arxiv.org/abs/1501.06858>.

- 193 [5] M. Abe *et al.* *A new approach for measuring the muon anomalous magnetic moment and*
194 *electric dipole moment*, Progress of Theoretical and Experimental Physics **2019**, 053C02
195 (2019), doi:[10.1093/ptep/ptz030](https://doi.org/10.1093/ptep/ptz030).
- 196 [6] S. Borsanyi *et al.* *Leading hadronic contribution to the muon magnetic moment from lattice*
197 *QCD*, Nature **593**, 51 (2021), doi:[10.1038/s41586-021-03418-1](https://doi.org/10.1038/s41586-021-03418-1).
- 198 [7] C. M. Carloni Calame, M. Passera, L. Trentadue, and G. Venanzoni *A new approach to*
199 *evaluate the leading hadronic corrections to the muon $g-2$* , Phys. Lett. B **746**, 325 (2015),
200 doi:[10.1016/j.physletb.2015.05.020](https://doi.org/10.1016/j.physletb.2015.05.020).
- 201 [8] G. Abbiendi *et al.* *Measuring the leading hadronic contribution to the muon $g-2$ via μe*
202 *scattering*, Eur. Phys. J. C **77**, 139 (2017), doi:[10.1140/epjc/s10052-017-4633-z](https://doi.org/10.1140/epjc/s10052-017-4633-z).
- 203 [9] G. Abbiendi *et al.* (MUonE Collaboration) *Letter of Intent: the MUonE project*, CERN-
204 SPSC-2019-026 / SPSC-I-252 (2019), <https://cds.cern.ch/record/2677471>.
- 205 [10] G. Abbiendi *et al.* *Results on multiple Coulomb scattering from 12 and 20 GeV electrons on*
206 *carbon targets*, JINST **15**, P01017 (2020), doi:[10.1088/1748-0221/15/01/p01017](https://doi.org/10.1088/1748-0221/15/01/p01017).
- 207 [11] M. Alacevich *et al.* *Muon-electron scattering at NLO*, J. High Energ. Phys. **02**, 155 (2019),
208 doi:[10.1007/JHEP02\(2019\)155](https://doi.org/10.1007/JHEP02(2019)155).
- 209 [12] M. Fael *Hadronic corrections to $\mu - e$ scattering at NNLO with space-like data*, J. High
210 Energ. Phys. **02**, 027 (2019), doi:[10.1007/JHEP02\(2019\)027](https://doi.org/10.1007/JHEP02(2019)027).
- 211 [13] M. Fael and M. Passera *Muon-Electron Scattering at Next-To-Next-To-Leading*
212 *Order: The Hadronic Corrections*, Phys. Rev. Lett. **122**, 192001 (2019),
213 doi:[10.1103/PhysRevLett.122.192001](https://doi.org/10.1103/PhysRevLett.122.192001).
- 214 [14] P. Mastrolia, M. Passera, A. Primo, and U. Schubert *Master integrals for the NNLO virtual*
215 *corrections to μe scattering in QED: the planar graphs*, J. High Energ. Phys. **2017**, 198
216 (2017), doi:[10.1007/JHEP11\(2017\)198](https://doi.org/10.1007/JHEP11(2017)198).
- 217 [15] S. Di Vita *et al.* *Master integrals for the NNLO virtual corrections to μe scat-*
218 *tering in QED: the non-planar graphs*, J. High Energ. Phys. **2018**, 16 (2018),
219 doi:[10.1007/JHEP09\(2018\)016](https://doi.org/10.1007/JHEP09(2018)016).
- 220 [16] S. Di Vita *et al.* *Master integrals for the NNLO virtual corrections to $q\bar{q} \rightarrow t\bar{t}$ scat-*
221 *tering in QCD: the non-planar graphs*, J. High Energ. Phys. **2019**, 117 (2019),
222 doi:[10.1007/JHEP06\(2019\)117](https://doi.org/10.1007/JHEP06(2019)117).
- 223 [17] R. Bonciani *et al.* *The two-loop four-fermion scattering amplitude in QED* (2021), <https://arxiv.org/abs/2106.13179>.
224
- 225 [18] C. M. Carloni Calame *et al.* *Towards muon-electron scattering at NNLO*, J. High Energ.
226 Phys. **2020**, 28 (2020), doi:[10.1007/JHEP11\(2020\)028](https://doi.org/10.1007/JHEP11(2020)028).
- 227 [19] P. Banerjee, T. Engel, A. Signer, and Y. Ulrich *QED at NNLO with McMule*, SciPost Phys. **9**,
228 027 (2020), doi:[10.21468/SciPostPhys.9.2.027](https://doi.org/10.21468/SciPostPhys.9.2.027).
- 229 [20] P. Banerjee *et al.* *Theory for muon-electron scattering @ 10 ppm*, Eur. Phys. J. C **80**, 591
230 (2020), doi:[10.1140/epjc/s10052-020-8138-9](https://doi.org/10.1140/epjc/s10052-020-8138-9).
- 231 [21] A. Masiero, P. Paradisi, and M. Passera *New physics at the MUonE experiment at CERN*,
232 Phys. Rev. D **102**, 075013 (2020), doi:[10.1103/PhysRevD.102.075013](https://doi.org/10.1103/PhysRevD.102.075013).

- 233 [22] P. B. Dev, W. Rodejohann, X. J. Xu, and Y. Zhang *MUonE sensitivity to new physics expla-*
234 *nations of the muon anomalous magnetic moment*, J. High Energ. Phys. **2020**, 53 (2020),
235 doi:[10.1007/JHEP05\(2020\)053](https://doi.org/10.1007/JHEP05(2020)053).
- 236 [23] CMS Collaboration *The Phase-2 Upgrade of the CMS Tracker*, CERN-LHCC-2017-009 /
237 CMS-TDR-014 (2017), <https://cds.cern.ch/record/2272264>.
- 238 [24] A. Rose *et al.* *Serenity: An ATCA prototyping platform for CMS Phase-2*, PoS **343**, 115
239 (2019), doi:[10.22323/1.343.0115](https://doi.org/10.22323/1.343.0115).